DRUG DELIVERY
2023, VOL. 30, NO. 1, 2165737
https://doi.org/10.1080/10717544.2023.2165737

Taylor & Francis
Taylor & Francis Group

RESEARCH ARTICLE

OPEN ACCESS Check for updates

Study of the permeation-promoting effect and mechanism of solid microneedles on different properties of drugs

Huahua Li, Ziwei Peng, Yang Song, Minhang Dou, Xinying Lu, Minghui Li, Xiaofeng Zhai, Yan Gu, Rexidanmu· Mamujiang, Shouying Du and Jie Bai

School of Traditional Chinese Medicine, Beijing University of Chinese Medicine, Beijing, China

ABSTRACT

In transdermal drug delivery systems, the physicochemical properties of the drug affect its percutaneous permeability. However, whether the physicochemical properties of drugs change their transdermal permeability in the presence of pores in the presence of solid microneedles (MNs) has been less studied in this area. In this project, cinnamaldehyde, curcumin, ferulic acid and geniposide were selected as model drugs for the study of their transdermal permeability under the action of MNs, and a combination of classical experiments and visualization means such as scanning electron microscopy and laser confocal was used to investigate the permeation-promoting mechanism of MNs. The results showed that the MNs had significant permeation-promoting effects on different properties of drugs, with the permeation-promoting effects on cinnamaldehyde, curcumin, ferulic acid and geniposide being 6.36, 17.43, 29.54 and 8.91 times, respectively, and the permeation-promoting effects were more pronounced for lipid-soluble and amphiphilic drugs. Using scanning electron microscopy, transmission electron microscopy and other means to confirm that MNs can promote the penetration by acting on the skin to produce pores, and their effect on skin structure is greater than that of drugs. In addition, the existence of pores increases the amount of drug transdermal, which may enhance the diffusion of drug on the skin, and has no effect on lipid exchange and transdermal route. Through the research, it has been found that MNs is equivalent to direct peeling of the stratum corneum (SC), but it is simpler and safer for the patient.

ARTICLE HISTORY
Received 9 November 2022
Revised 27 December 2022
Accepted 2 January 2023

KEYWORDS
Solid microneedles; different properties of drugs; promoting permeation; mechanism

1. Introduction

Transdermal Drug Delivery System (TDDS) is a noninvasive drug delivery method that has many advantages over oral and injectable drug delivery, including: reducing toxicity, avoiding first pass effect, improving bioavailability, prolonging dosing time, reducing the number of doses and improving patient compliance, making it an important delivery route for a variety of local or systemic therapeutic agents (Prausnitz & Langer, 2008; Marwah et al., 2016). However, the dense stratum corneum (SC) of the skin (Parhi et al., 2015) prevents most drugs from being absorbed transdermally to achieve effective blood concentrations, and then resulting in an unexpected therapeutic effect. Therefore, how to enhance the penetration of drugs in the skin and improve their bioavailability has become a difficult and important point in the research and development of transdermal drug delivery formulations.

Current methods for promoting transdermal absorption include physical methods such as ion introduction (Abla et al., 2005), electroporation (Chang et al., 2000), ultrasound introduction (Mitragotri & Kost, 2004; Seah & Teo, 2018); Nano-carrier methods such as microemulsions, nanoparticles, liposomes (Marwah et al., 2016); Chemical methods to modify the chemical structure of drugs to synthesize precursors with higher transdermal rates, and chemical agents such as nitrogen ketones, ethanol, propylene glycol and volatile oils of Chinese herbs (Kováčik et al., 2020; Sarango-Granda et al., 2022).

Solid microneedles (MNs), as a minimally invasive and painless physical means of promoting osmosis (Guillot et al., 2020) are also used widely in transdermal drug delivery. MNs is small in size and typically range in length from a few tens to hundreds of microns. Skin anatomy shows that MNs can penetrate the 10 ~ 20 μm thick SC and reach the superficial dermis. A large number of capillaries in the dermis facilitates the penetration of drugs into the human circulatory system through the micron-sized channels created by MNs in the skin, overcoming the barriers to effective drug penetration (Bariya et al., 2012; Riemma Pierre & Rossetti, 2014). Although the micro-permeation effect is stronger against large molecules, it is also widely used to promote the permeation of small molecules (Waghule et al., 2019; Mdanda et al., 2021). Due to the different nature of the drug, the permeation

CONTACT Jie Bai baijie22811@163.com School of Traditional Chinese Medicine, Beijing University of Chinese Medicine, Yangguang South Street, Fangshan District, Beijing, 102488, China

variability in transdermal delivery (Xie et al., 2016; Chen et al., 2020) and the facilitation of transdermal permeation by MNs varies with the nature of the drug. Although the use of MNs is becoming increasingly widespread, there are no systematic studies on the facilitation of percutaneous permeation of different drugs by MNs and the related mechanisms. How solid MNs play their role in the transdermal administration of different drugs and their effect on skin structure and drug penetration pathways are questions that need to be investigated.

Based on this, this paper systematically investigates the permeation-promoting effect and mechanism of solid MNs for different properties of drugs. Using the logP of the drug as the main indicator, four drug components commonly found in the transdermal drug delivery field were selected for the correlation between their permeability and drug properties, and the drug information is shown in Table 1. These drugs are small molecules with molecular weights (MW) below 500; their polarities cover water-soluble, amphiphilic and lipid-soluble. After examining the permeation of these model drugs, the permeation-promoting effect and transdermal permeation pattern of solid MNs on different properties of model drugs were further investigated. Based on the polarity of four model drugs, one water-soluble, amphiphilic and lipid-soluble drug and fluorescent substances were each selected, and the permeation-promoting mechanism of MNs was explored using a combination of classical experiments and visualization means such as scanning electron microscopy and laser confocal. The above study enables a systematic analysis of the role of MNs in the promotion of permeation of drugs of different properties and facilitates the development of transdermal drug delivery formulations. The study is also a systematic study of the mechanism of microneedle permeation promotion, which is of great significance for the application of MNs in clinical practice.

2. Materials and methods

2.1. Materials

Sartorius BSA 224S electronic analytical balance (Sartorius Scientific Instruments (Beijing) Co., Ltd.); High Performance Liquid Chromatography (HPLC, Agilent 1100, Agilent Technologies Ltd.); Vortex (MS-X, DragonLab); Ultrasonic cleaner (SB25-12DTD, Ningbo Xinling Biotechnology Co., Ltd.); TK-121 Drug Transdermal Diffusion Tester (Tianjin Zhengtong Technology Co., Ltd.); DRS Dermaroller 600 roller microneedle (Guangzhou Mingmo Trading Co., Ltd.); Laser confocal fluorescence microscope (NIKON ECLIPSE TI, Nikon, Japan); Cryostat (CryoStar NX50, Thermo Fisher); Scanning Electron Microscope (SEM) (Nova Nano 450); Octane EDS-70 (silicon nitride) critical point dryer (Leica CPD300, Germany); Transmission Electron Microscope (TEM) (Hitachi H-7650); Ultra-thin sectioning machine (Leica UC7).

Table 1. LogP of model drugs.

Model drugs	log P	MW
Curcumin	3.62	368.38
Cinnamaldehyde	1.98	132.16
Ferulic acid	1.58	194.184
Geniposide	1.92	388.366

Methanol, acetonitrile, acetic acid, phosphoric acid (Fisher, chromatographically pure); Controls were purchased from China Institute of Food and Drug Control: Cinnamaldehyde (Batch No. 110710-202022, 99.5% purity); Curcumin (Batch No. 110823-202107, 98.1% purity); Ferulic Acid (Batch No. 110773-201915, 99.4% purity) (Batch No. 110773-201915, 99.4% purity); Geniposide (Batch No. 110749-201919, 97.1% purity). Ltd. All raw materials are purchased from Shanghai Yuanye Biotechnology Co: Geniposide (purity ≥ 98%); Curcumin (purity ≥ 95%); Ferulic acid (purity ≥ 99%); Cinnamaldehyde (purity ≥ 95%); anhydrous ethanol (Beijing Chemical Factory, analytical purity), polyethylene glycol-400, 1,2-propanediol (Sinopharm Chemical Reagent Co., Ltd., analytical purity), Polydimethylsiloxane (PDMS) film (Hangzhou Wiskind Technology Co., Ltd., thickness: 100 μm), 0.2 μm microporous filter membrane (Tianjin Jinteng Experimental Equipment Co., Ltd.).

Male Kun Ming (KM) mice (20 ± 1 g), supplied by Spelford (Beijing) Biotechnology Co., Ltd, Certificate of Conformity No. SCXK (Beijing) 2019-0001.

2.2. Transdermal permeability studies of different model drugs

2.2.1. Preparation of the test solution

Weigh appropriate amounts of curcumin, cinnamaldehyde, ferulic acid and geniposide, respectively, in a 25 mL volumetric flask, add solvent (propylene glycol-water = 8:2) to fix the volume, vortex treatment for 5 min, sonicate for 15 min to dissolve the drugs, i.e. 0.5 mg·mL^{-1} of the test solution.

2.2.2. Preparation of isolated skin

Male KM mice were taken, cervicalized and executed. After shaving the abdomen with a shaver, a layer of hair removal cream was evenly applied, left for 1 min and then wiped off to completely remove the abdomen hair, ensuring that the cuticle was intact, separate the abdominal skin, remove the fatty and connective tissue with skimmed cotton and rinse well with saline Wrap in aluminum foil and store frozen at −20 °C, use up within a week.

2.2.3. Franz's diffusion cell method

The isolated skin prepared in Section 2.1.1 was naturally thawed and set aside. An 8 mL transdermal diffusion cell was used, and the rat skin was fixed between the supply and receiving chambers of the transdermal diffusion cell with the SC facing the supply chamber (effective diffusion area 3.14 cm^2). 8 mL of transdermal receiving solution (polyethylene glycol 400-ethanol-saline = 3:3:4) was added separately to the receiving cell, which was equipped with a built-in magnetic stirrer and maintained at a constant speed of 350 r·min^{-1} and a constant temperature of (37 ± 0.5) °C. After the air bubbles in the receiving cell were completely expelled,

2 mL of the test solution was added to the supply chamber, respectively, and the transdermal diffusion cell was placed in the transdermal apparatus and 1 mL was sampled at 5 min, 15 min, 30 min, 60 min, 90 min, 120 min, 180 min, 240 min, 300 min and 360 min, respectively, while an equal volume of the same temperature of the fresh reception solution was added at the same time. The sample was filtered through a 0.45 μm microporous membrane and determined by HPLC according to the above chromatographic method.

The solid MNs used in the experiments were commercially available, and the microneedle bodies were metal MNs prepared from titanium alloy, with 10 rows of 60 needles each. The transdermal medium used for the study of percutaneous permeability of model drugs under MNs action was the skin of microneedle-treated mice. Microneedle conditions (Yang et al., 2021) were based on efficacy and safety, combined with preliminary laboratory studies using a 250 μm microneedle matrix (including handle) applied with a force of 5 N, the thawed skin was fixed on a potato slice and then placed on electronic balance, (1 N pressure corresponds to 100 g on balance, the MNs were balanced while rolling to keep the balance within ± 20% error) and rolled at 30 times/min for 2 min over the effective drug delivery area. The treated skin was immediately fixed in the diffusion cell for transdermal experiments.

2.2.4. Comparison of transdermal permeability results for different models of drugs

The cumulative transmissible amount (Q_n) and transdermal rate (J_{ss}) of each model drug at their corresponding times were calculated according to the following equation (1).

$$Q_n = (VC_n + 1.0 \times \sum_{i-1}^{n-1} C_i) / S \quad (1)$$

The formula Q_n is the cumulative permeation per unit area (μg) at the nth time point, V is the volume of the receiving fluid (8 mL), C_n is the concentration of the receiving fluid at the sampling point (μg · mL^{-1}), and S is the effective area of the diffusion cell (3.14 cm^2).

The cumulative transmissible amount Q_n is the vertical coordinate and time T is the horizontal coordinate to obtain the cumulative transmissible amount - time curve of the drug, a linear regression can be performed to obtain the pharmacokinetic equation $Q_n = J_{ss} \times T + B$ for each model, the slope of the linear part (120 ~ 360 min) is the transdermal rate J_{ss} (μg·cm^{-2}·h^{-1}), the intersection of the reverse extension of the linear part with the X-axis is the lag time T_{log} (min).

The permeation enhancement factor (ER) can be calculated according to the following equation (2) to explore the permeation-promoting ability of microspheres for different model drugs.

$$ER = J_e / J_0 \quad (2)$$

where J_e is the transdermal rate after the addition of the MNs action and J_0 is the transdermal rate without the addition of the MNs action.

2.3. Mechanistic studies on the promotion of drug penetration by microneedling

2.3.1. Distribution of drugs of different properties in the skin

In this experiment, fluorescein sodium, coumarin 6 and nile red, which can show fluorescence, were selected as representatives of water-soluble, amphiphilic and lipid-soluble drugs, the properties of which are shown in Table 2, to study the distribution of drugs in the skin before and after the action of MNs. After 60 mins of transdermal penetration of the fluorescent representatives under normal conditions and in the presence of MNs, respectively, the excess drug solution was removed from the skin surface, the skin was removed and stored at −80 °C.

The skin was stained with the immunofluorescent dye -4,6-diamidino-2 -phenylindole (DAPI), which binds to DNA in the nucleus and appears blue at 365 nm. Fluorescein sodium and coumarin 6 fluoresced green at 365 and 545 nm respectively, and nile red fluoresced red at 530 nm. Thus, the fluorescence of the representatives and DAPI can be used to assess the depth of microtargeting to the drug's transdermal depth and the distribution of the different properties of the drug in the skin. Finally, the frozen sections were observed under a laser confocal microscope.

2.3.2. Effect of MNs and drugs on the surface morphology of the SC

This experiment used scanning electron microscopy to observe the changes of MNs and different nature of drugs on the surface of mouse skin SC. The skin of the model drugs curcumin, ferulic acid and geniposide with and without microneedle action after in vitro percutaneous penetration experiments, control and blank control groups were cut into 1 mm x1 mm squares, respectively. The skin was then washed 3 times with PBS (pH 7.4) buffer, washed and placed in 2.5% glutaraldehyde fixative and transferred to 2 ~ 8 °C refrigerator overnight for primary fixation.

Skin samples were removed from the glutaraldehyde fixative and rinsed three times for 15 min each with 0.1 mol·L^{-1} PBS (pH 7.4) buffer. The rinsed skin tissue was post-fixed with 1% osmium solution for 1 to 2 h. At the end of this time, the skin was rinsed three times for 15 min each with 0.1 mol·L^{-1} PBS (pH 7.4) buffer.

The samples were dehydrated with graded concentrations of ethanol (30%, 50%, 70%, 80%, 90%, 95%) for 15 min per gradient and then twice with 100% ethanol for 20 min each. 30 min were treated with a mixture of ethanol and isoamyl acetate (V/V = 1/1) and then pure isoamyl acetate for 1 h or left overnight. After critical point drying, the samples were

Table 2. Properties of fluorescent markers.

Name	Solubility	MW	Wavelength	Fluorescent color
Fluorescein sodium	Water-soluble	376.27	365 nm	Green
Coumarin 6	Amphiphilic	350.43	545 nm	Green
Nile red	Lipid-soluble	318.37	530 nm	Red

ion sputter coated and finally the treated skin samples were observed in a scanning electron microscope.

2.3.3. Effect of MNs and drugs on skin structure

In this experiment, transmission electron microscopy was to observe the alteration of the skin structure of mice by microneedling and different nature of drugs. The skin of the model drugs curcumin, ferulic acid and geniposide with and without microneedle action after in vitro percutaneous penetration experiments, control and blank control groups were cut into 1 mm x 1 mm squares, respectively. The skin was then washed 3 times with PBS (pH 7.4) buffer, washed and placed in 2.5% glutaraldehyde fixative and transferred to a refrigerator at 2–8 °C overnight for primary fixation. The skin samples were removed from the glutaraldehyde fixative and rinsed 3 times for 15 min each with 0.1 mol·L^{-1} PBS (pH 7.4) buffer. The rinsed skin tissue was post-fixed with 1% osmium solution for 1 to 2 h. At the end of this time, the skin was rinsed 3 times for 15 min each with 0.1 mol·L^{-1} PBS (pH 7.4) buffer.

The samples were dehydrated with a graded concentration of ethanol (30%, 50%, 70%, 80%, 90%, 95%) for 15 min in each gradient and then with 100% ethanol for 20 min. The samples were then treated with a mixture of embedding agent and acetone (V/V = 1/1) for 1 h followed by a mixture of embedding agent and acetone (V/V = 3/1) for 3 h. The samples were treated with pure embedding agent overnight and then the permeabilized samples were embedded and heated at 70 °C overnight to obtain the embedded samples. Sections of 70 ~ 90 nm were obtained, stained with lead citrate solution and 50% ethanol saturated uranyl acetate for 5 ~ 10 min each, dried and ready for observation in the transmission electron microscope.

2.3.4. Permeation of drugs with different properties in the pore channel

In this experiment, we studied the permeation of drugs with different properties in the pore channels. To avoid chance results after one diffusion medium simulating pore channel experiments, we chose microporous filter membranes and PDMS membranes that have almost no permeation effect on the drug for the experiments. PDMS film is a polymeric membrane material made of polydimethylsiloxane raw material, which has excellent biocompatibility, heat resistance and low-temperature flexibility, and is almost impermeable to drugs. The 0.2 μm microporous filter membrane and PDMS film after MNs action were used as diffusion media, and the MNs action conditions were the same as those of the treated mouse skin, and the rest of the procedure was the same as in Section 2.1.3.

2.3.5. Lipid exchange of drugs with different properties

Starting from the basis of microporous filter membrane and PDMS film studies, it was verified whether the lipid exchange effect is the main cause of drug permeation differences. Start-M membranes are commercially available artificial membranes that can replace the skin and have a structural composition that mimics skin lipids, which is not found in microporous membranes and PDMS membranes, so Start-M membranes were chosen as the diffusion medium for the experiments (Haq et al., 2018; Kovács et al., 2021), and the rest of the procedure was the same as in Section 2.1.3.

2.4. Mechanistic studies of skin in differential drug penetration

2.4.1. Penetration of different properties of drugs in exfoliated skin

In this experiment, the penetration of drugs on the skin with the removal of the SC was investigated. Spare isolated mouse skin was removed by tape stripping to remove the SC (Benfeldt, 1999; Cadavona et al., 2016), 20 times to ensure complete SC removal, wrapped in aluminum foil and stored frozen at −20 °C for use within one week.

2.4.2. Distribution of different properties of drugs in the SC

The skin of isolated mice was placed in 0.25% (W/V) trypsin solution and left at room temperature for about 10 h. The skin cuticle was then carefully separated with cotton swabs, and the obtained cuticle pieces were rinsed with water and dried in a vacuum oven at 37 °C for 6 h. The dried skin cuticle was ground and grinded, weighed about 20 mg in a 10 mL EP tube, and 1 mL of drug-containing solution (curcumin, ferulic acid and geniposide) (0.5 mg·mL^{-1}), vortexed and mixed, placed in a constant temperature water bath at 37 °C for 12 h, centrifuged at 10000 rpm for 10 min, and the supernatant was appropriately diluted and injected according to the HPLC method for determination of drug content. The amount of drug added minus the amount of drug in the solvent was determined as the drug content in the cuticle and each group was operated three times in parallel (Xie et al., 2016). The partition coefficient (K) of the drug in the SC to the medium was calculated according to Eq. (3) as follows:

$$K = \frac{C_{(SC)}}{C_{(vehicle)}} \tag{3}$$

where $C_{(SC)}$ and $C_{(vehicle)}$ are the drug concentration in the SC and medium (i.e. supernatant), respectively.

3. Results and discussion

3.1. MNs promote transdermal permeability of drugs in different models

The results of transdermal permeation of each model drug under without (Figure 1) and with (Figure 2) MNs were cinnamaldehyde > ferulic acid > curcumin > geniposide. Statistical analysis by SPSS 20 for the cumulative transdermal permeation Q_n of each model drug with and without microneedlles action, the results showed that $P < 0.05$, all statistically significant, indicating that MNs action can significantly promote the transdermal permeation of each model drug (Figure 3).

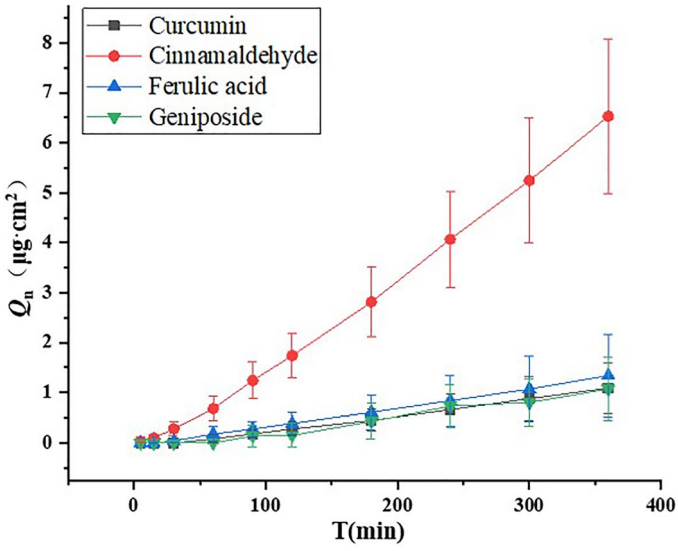

Figure 1. Cumulative transdermal permeation-time curves for different models of drugs without microneedle action over 6 h ($n = 6$).

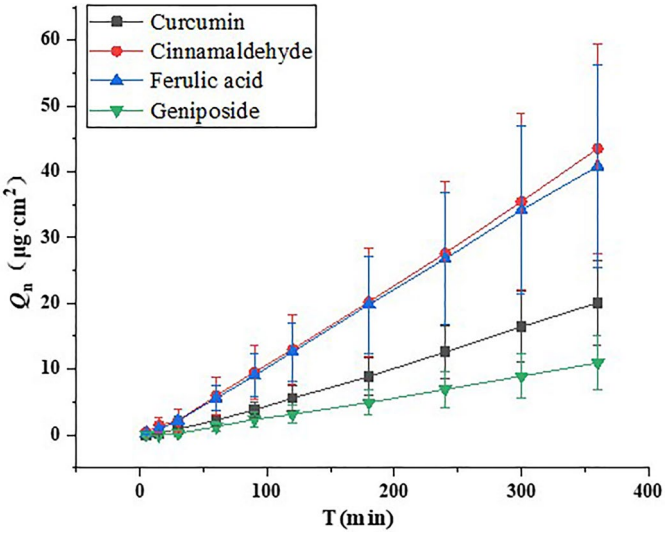

Figure 2. Cumulative transdermal permeation-time curves for different models of drugs under microneedle action over 6 h ($n = 6$).

Moreover, the results showed that microneedle action promoted the permeation of curcumin and ferulic acid by 17.43-fold and 29.54-fold, respectively as shown in Table 3, indicating that microneedle action promoted the permeation of strongly lipid-soluble and amphiphilic drugs more.

3.2. Correlation between the transdermal properties of model drugs and drug properties

3.2.1. Correlation between transdermal properties and drug logP

The correlation between the logP values (−1.92 to 3.62) of each model drug and the transdermal rate J_{ss} within 6 h with or without MNs was performed by SPSS 20 (Figure 4).

The results of the quadratic polynomial regression showed that the correlation regression equation between the rate of drug transdermal penetration without MNs and the logP value was: $J_{ss} = -0.064\text{logP}^2 + 0.124\ \text{logP} + 0.678$ ($r = 0.537$, $P = 0.843$); the correlation regression equation between the rate of drug transdermal penetration with MNs and the logP value was: $J_{ss} = -0.621\text{logP}^2 + 1.377\text{logP} + 6.878$ ($r = 0.991$, $P = 0.132$). The results of the analysis showed that the drug transdermal rate was roughly parabolic with the lipophilicity of the drug with and without MNs action. In other words, the drug transdermal rate tends to increase and then decrease with its lipid solubility. It indicates that suitable drug lipophilicity is more favorable for transdermal penetration of drugs, which is consistent with the literature (Lan et al., 2016). Moreover, it can be seen that the correlation between the transdermal permeation rate of the drug and the logP value tends to be more pronounced after the addition of MNs. Because in the absence of MNs, the model drug cinnamaldehyde is a volatile oil component, which itself has a pro-permeability effect, its transdermal permeation rate is more than five times higher than that of other model drugs, and the difference is larger. In

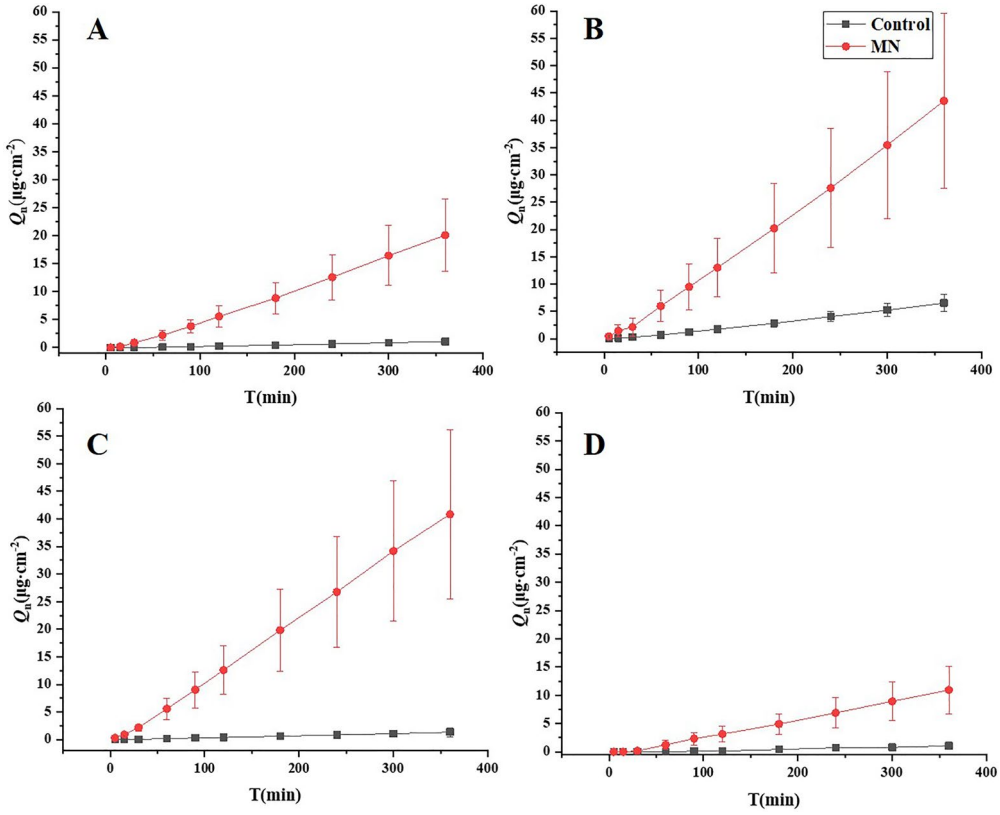

Figure 3. 6 h in vitro transdermal permeation curves of model drugs with and without microneedle action ($n = 6$). (A) Curcumin; (B) Cinnamaldehyde; (C) Ferulic acid; (D) Geniposide.

Table 3. 6 h in vitro transdermal permeation parameters of model drugs with and without microneedle action ($n = 6$).

Drug	Group	logP	Osmodynamic equations	r	Q_n (μg·cm^{-2})	J_{ss} (μg cm^{-2}·h^{-1})	T_{log} (min)	ER
Curcumin	Blank	3.62	Q_n = 0.0031T − 0.0789	0.9963	1.09 ± 0.50	0.21 ± 0.10	44.59 ± 12.57	17.43
	MNs		Q_n=0.0572T − 0.9481	0.9985	20.09 ± 6.46	3.66 ± 1.19	30.87 ± 10.24	
Cinnamaldehyde	Blank	1.98	Q_n = 0.0184T − 0.3058	0.9977	6.53 ± 1.55	1.20 ± 0.29	35.58 ± 12.98	6.36
	MNs		Q_n=0.1216T − 1.0929	0.9992	43.55 ± 15.95	7.63 ± 2.66	22.62 ± 10.73	
Ferulic acid	Blank	1.58	Q_n= 0.0038T − 0.0556	0.9991	1.34 ± 0.83	0.24 ± 0.16	42.34 ± 20.01	29.54
	MNs		Q_n=0.1163T − 1.0709	0.9997	40.85 ± 15.35	7.09 ± 2.73	11.38 ± 7.39	
Geniposide	Blank	−1.92	Q_n = 0.0031T − 0.1089	0.9841	1.07 ± 0.63	0.22 ± 0.10	77.20 ± 46.39	8.91
	MNs		Q_n=0.0314T − 0.534	0.9989	10.95 ± 4.17	1.96 ± 0.70	27.94 ± 10.35	

contrast, MNs has a better ability to promote the permeability of curcumin and ferulic acid, which have poor permeability themselves, allowing the model drugs to have a tendency to converge in permeability under MNs, which makes the correlation between drug permeation rate and logP with and without MNs different.

3.2.2. Correlation between transdermal properties and drug MW

The correlation between the MW values of each model drug and the transdermal rate J_{ss} within 6 h with or without MNs was performed by SPSS 20 (Figure 5).

The linear regression results showed that the correlation between drug transdermal penetration rate and drug molecular weight without MNs was J_{ss} = −0.003 MW + 1.241 (r = 0.743, $P = 0.257$, F = 2.464); the correlation between drug transdermal rate and drug MW with MNs was J_{ss} = −0.021 MW + 10.748 (r = 0.975, $P = 0.025$, F = 38.137). The results of the analysis showed that the drug transdermal rate was linearly correlated with the molecular weight of the drug with and without MNs action. The result means that the rate of drug transdermal transmission decreases as its MW increases, indicating that drugs with smaller MW are more likely to pass through the skin when administered transdermally under normal conditions. Similarly, because the transdermal rate of cinnamaldehyde was higher than that of other model drugs, the correlation between the transdermal permeation rate of drugs and MW trended more clearly after the addition of MNs. And the MW of curcumin and ferulic acid, which have good microneedle permeation-promoting ability, were not among the two similar model drugs, indicating that microneedle targeting different molecular weights is not specific to the large or small molecule drugs among them.

In summary, the correlation between drug percutaneous penetration rate and logP value as well as MW was more obvious after adding MNs, suggesting that MNs action breaks

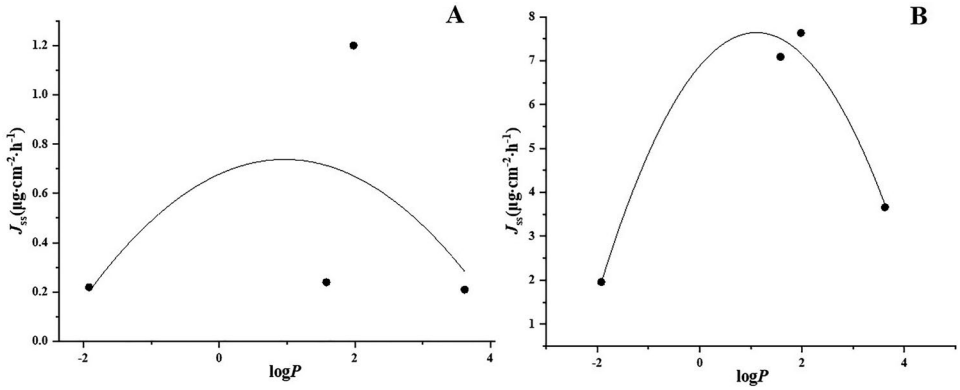

Figure 4. Correlation between drug transdermal rate and logP value ((A) without microneedle; (B) with microneedle).

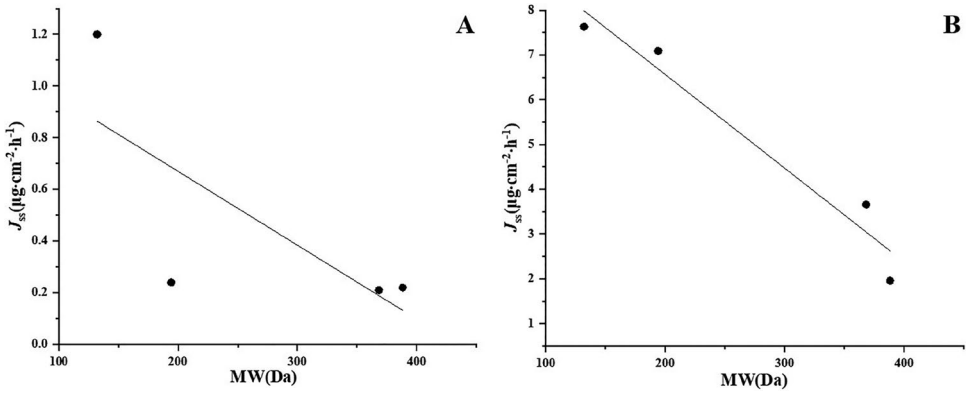

Figure 5. Correlation between drug transdermal rate and MW values ((A) without microneedle; (B) with microneedle).

the barrier effect of the SC, which makes some drugs better penetrate the SC, and highlights the influence of common characteristics of lipophilicity and MW of drugs on their percutaneous penetration performance.

3.3. Mechanistic studies on the promotion of drug penetration by MNs

3.3.1. Distribution of drugs of different properties in the skin

From the overall view of the results, the drug fluorescence intensity of the microneedle group (Figures 6(D), 7(D), and 8(D)) was higher than that of the blank group (Figures 6(A), 7(A), and 8(A)) in the 3 groups of experiments, and it was obvious that the fluorescence intensity of the inner side of the skin was also high in the microneedle group, indicating that the microneedle has a better promotion effect on the transdermal penetration of the drug. It can be observed that the normal group (Figures 6(A), 7(A), and 8(A)) had occasional curved corrugations on the SC with an intact structure and a very flat surface. In contrast, the experimental group (Figure 6(D), 7(D), and 8(D)) with MNs action had some folds and indentations on the surface of the SC, and even more so, the SC was broken at individual places, indicating that the microneedle treatment would destroy the intact structure of the SC and thus the drug could penetrate more into the skin for the purpose of promoting permeation.

Under normal conditions, the pathways of transdermal penetration of drugs may vary depending on the nature of the drug and the composition of the skin (Barbero & Frasch, 2006; Montenegro et al., 2016; Haque & Talukder, 2018). Whereas the differences in drug permeation pathways can be further reflected by their distribution in the skin, then whether MNs action affects the distribution of drugs in the skin. From the laser confocal microscopy results of sodium fluorescein permeation experiments (Figure 6), DAPI was staining the cells, while the drug fluorescence in the normal group (Figure 6(C)) and microneedle group (Figure 6(F)) was basically the same as the fluorescence site of DAPI, indicating that the fluorescent substance sodium fluorescein was mainly distributed in the cells. Sodium fluorescein has good water solubility, and it is presumed that the water-soluble drug is mainly distributed in the cells after entering the skin, and the MNs action almost does not affect the distribution of the water-soluble drug in the skin. In the laser confocal microscopy results of coumarin 6 (Figure 7) and nile red (Figure 8) permeation experiments, drug fluorescence was shown in both normal (Figures 7(F) and 8(F)) and microneedle groups (Figures 7(F) and 8(F)) at fluorescent sites with and without DAPI, and coumarin 6 and nile red are amphiphilic and lipid-soluble substances, respectively, indicating that amphiphilic and lipid-soluble drugs are more distributed intracellularly and intercellularly (Barry & Bennett, 1987; Yang et al., 2017). In addition, the fluorescence intensity of coumarin 6 and nile red in the microneedle group was higher than that in the normal group, but the fluorescence

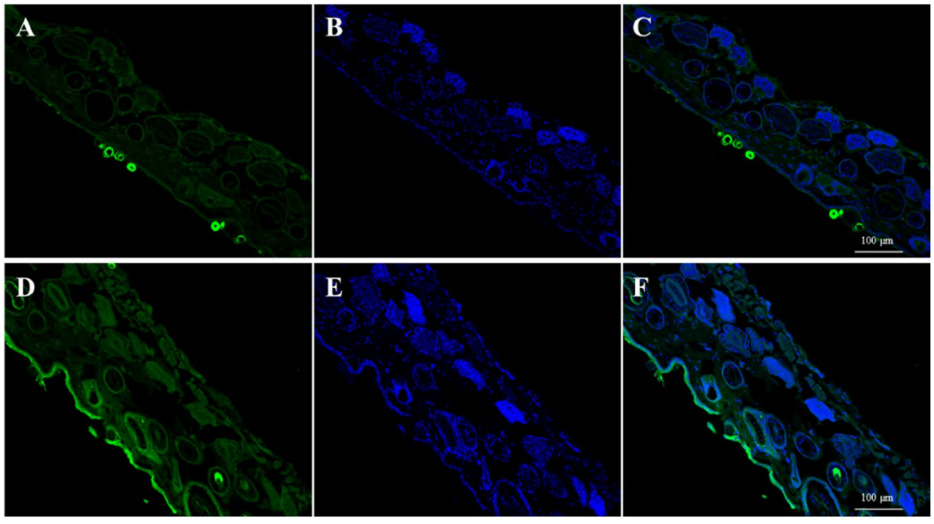

Figure 6. Laser confocal microscopy of percutaneous skin penetration with sodium fluorescein (Blank (A) Fluorescein sodium; (B) DAPI; (C) Fluorescein sodium + DAPI; MNs (D) Fluorescein sodium; (E) DAPI; (F) Fluorescein sodium + DAPI).

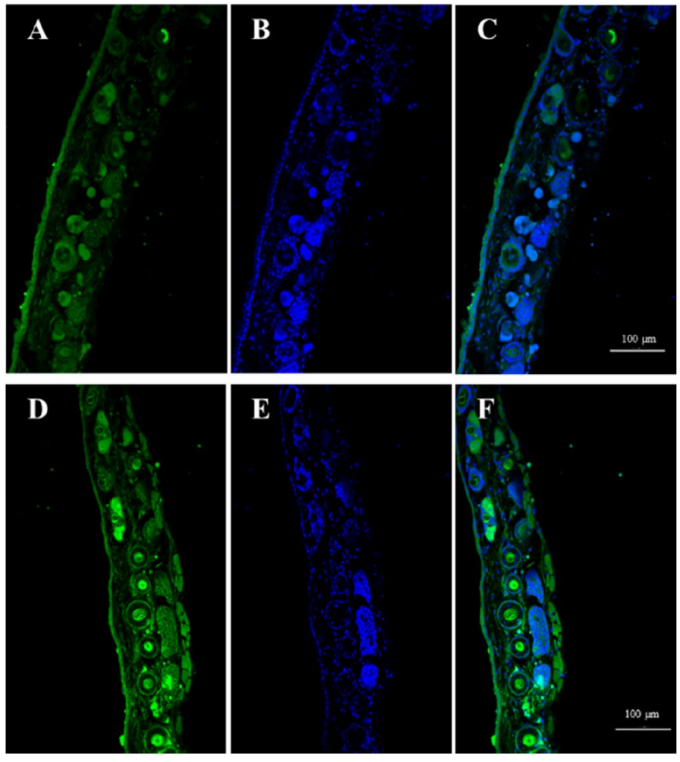

Figure 7. Coumarin 6 percutaneous penetration of the skin by laser confocal microscopy (Blank (A) Coumarin 6; (B) DAPI; (C) Coumarin 6 + DAPI; MNs (D) Coumarin 6; (E) DAPI; (F) Coumarin 6 + DAPI).

distribution sites were not significantly changed, which is also an indication that microneedle does not change the distribution of amphiphilic and lipid-soluble drugs in the skin. However, compared with the sodium fluorescein microneedle group, it can be seen that the increase of its fluorescence intensity compared with the normal group is not as obvious as the increase of fluorescence intensity of coumarin 6 and nile red, which is consistent with the better pro-permeation effect of microneedle on amphiphilic and lipid-soluble drugs.

Looking at the transdermal depth in terms of fluorescence intensity of different substances, the drug in the microneedle group was more concentrated at 28.5 ~ 100 μm, whereas the drug in the normal group was more evenly distributed at different depths. Pre-laboratory studies found that the micropore channel depth was 46.95 μm when the skin was treated with the microneedle conditions used in this paper, and the pore channel depth was 4.69 μm after 60 min of recovery (Yang et al., 2021). It can therefore be seen that the drug enters the skin through the channels left in the skin after the action of the microneedle, and that the barrier effect of the SC is diminished during transdermal action. Taken together, the results of this experiment indicate that the MNs

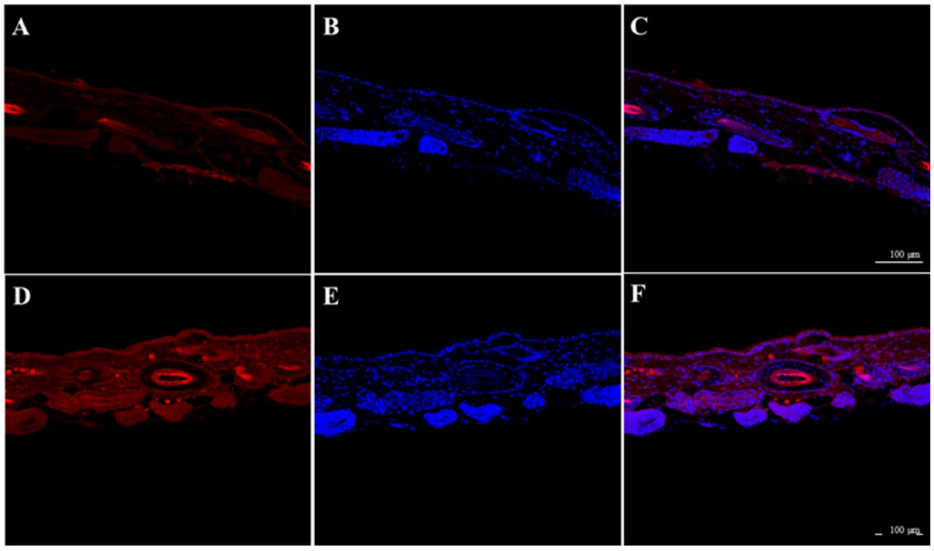

Figure 8. Nile red transdermal penetration of the skin as observed by laser confocal microscopy (Blank (A) Nile Red; (B) DAPI; (C) Nile Red + DAPI; MNs (D) Nile Red; (E) DAPI; (F) Nile Red + DAPI).

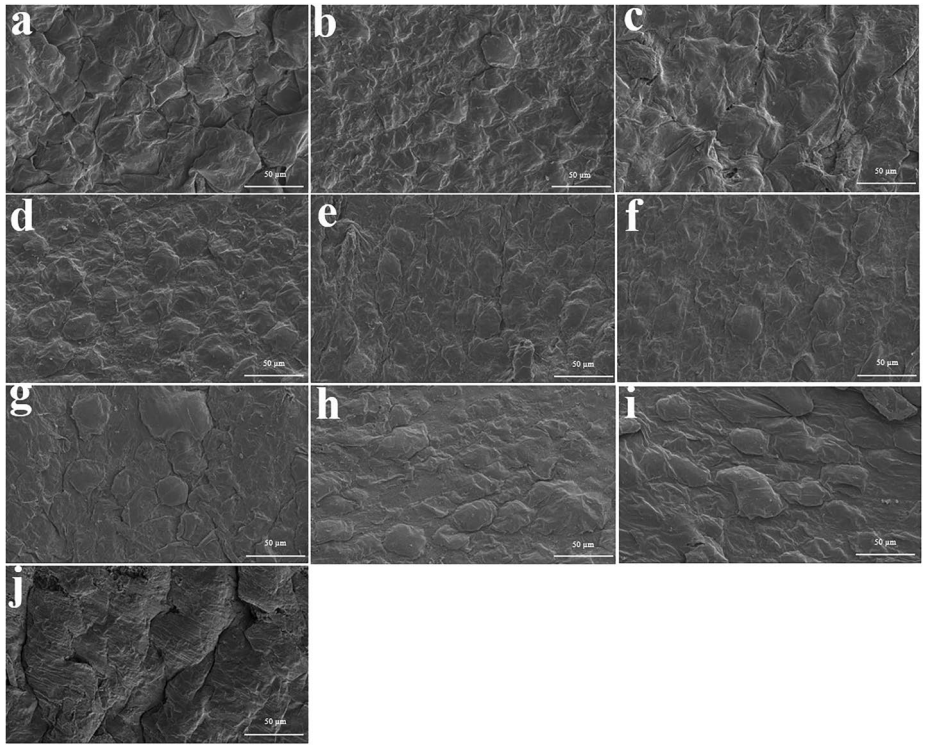

Figure 9. Scanning electron microscopy results of skin morphology with and without MNs for different drug effects ((A) Blank group; (B) Solvent group; (C) MNs (6 h); (D) Geniposide; (E) Ferulic acid; (F) Curcumin; (G) MNs + Geniposide; (H) MNs + Ferulic acid; (I) MNs + Curcumin; (J) MNs (0 h)).

only has a pro-permeation effect on the drug and does not change its distribution in the skin.

3.3.2. Effect of MNs and drugs on the surface morphology of the SC

Transdermal permeation of drugs under microneedle action is the direct action of the drug on the surface of the skin after MNs treatment, which is absorbed through the skin and then enters the body circulation to play a role. However, there are differences in the percutaneous permeability of different drugs under the action of MNs to promote permeation, based on which the effect of microneedle action and different nature of drugs on the skin surface structure was observed by scanning electron microscopy. The experimental results showed (Figure 9) that the structures on the surface of the skin samples in the blank group were more regularly protruding, the protruding structures were probably SC cells and the boundaries between each protrusion were clearer and more distinct. In the solvent group, nearly half of the protrusions disappeared and the skin surface became flat, but there were many folds where the protrusions had

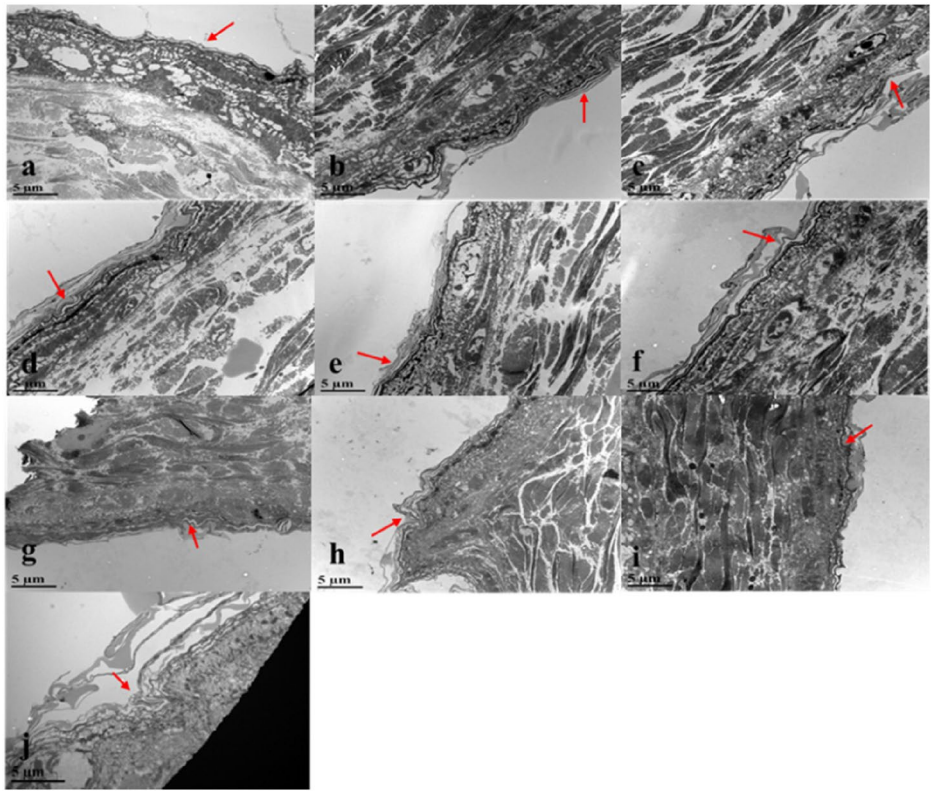

Figure 10. Transmission electron microscopy results of skin morphology with and without MNs for different drug effects ((A) Blank group; (B) Solvent group; (C) MNs (6 h); (D) Geniposide; (E) Ferulic acid; (F) Curcumin; (G) MNs + Geniposide; (H) MNs + Ferulic acid; (I) MNs + Curcumin; (J) MNs (0 h)).

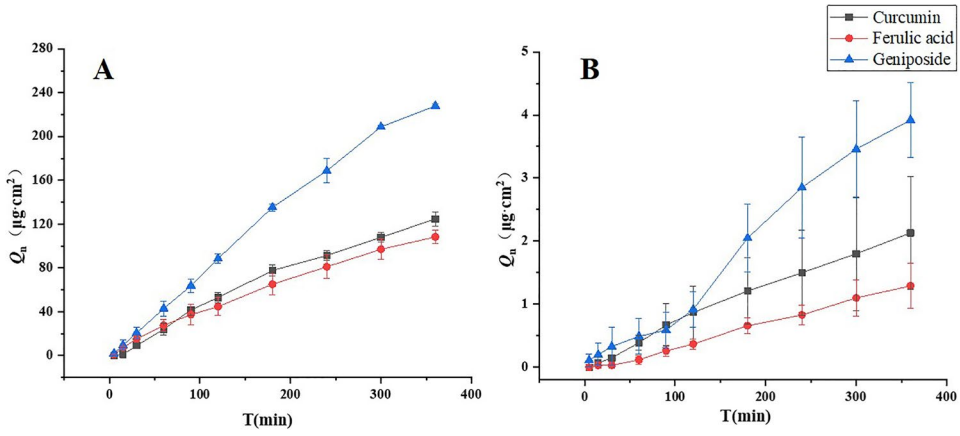

Figure 11. Permeation curves of model drugs with different properties in the pore channel ($n = 3$) ((A) 0.2 μm microporous filter membrane; (B) PDMS membrane).

disappeared, and there were fewer obvious boundaries between the protrusions, indicating that the solvent had some effect on the skin surface structure. In the microneedle group, a more serious breakage of the skin surface was evident at 0 h, indicating that the microneedle action disrupted the intact structure of the SC, which was responsible for its facilitation of transdermal drug penetration. In contrast, at 6 h the surface of the skin samples of the microneedle group could clearly see that the boundaries of the protrusions had basically disappeared completely, and a comparison with the 0 h skin showed that there were some traces of breakage on its surface, indicating that the skin surface was also gradually recovering during the 6 h transdermal permeation. The surface of the skin samples after transdermal penetration of different drugs also showed slight changes, the surface of the skin samples in the geniposide group was most similar to that of the solvent group, indicating that the drug in the geniposide group had less effect on the skin structure; the surface of the skin samples in the curcumin and ferulic acid groups was flatter and smoother than that of the geniposide group. After microneedling, traces of disruption of the skin surface SC were evident in the geniposide, ferulic acid and curcumin group, but there was no significant difference in structure between the drug groups, indicating that the effect of MNs on the surface structure was greater than that of the drugs.

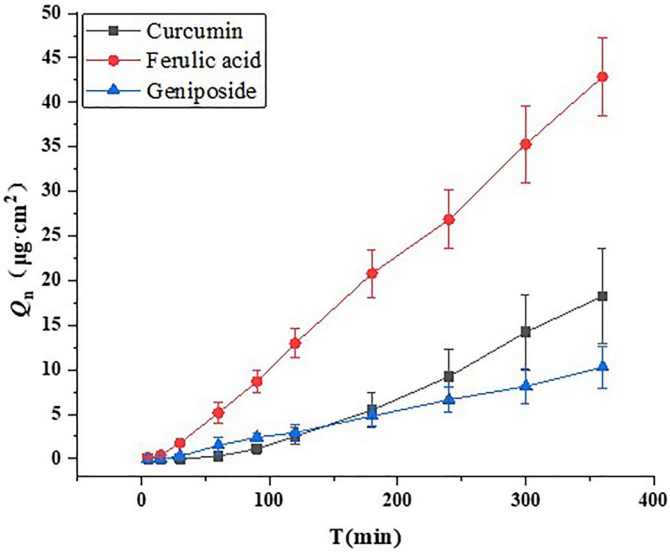

Figure 12. Permeation curves of model drugs with different properties in Start-M membranes ($n = 3$).

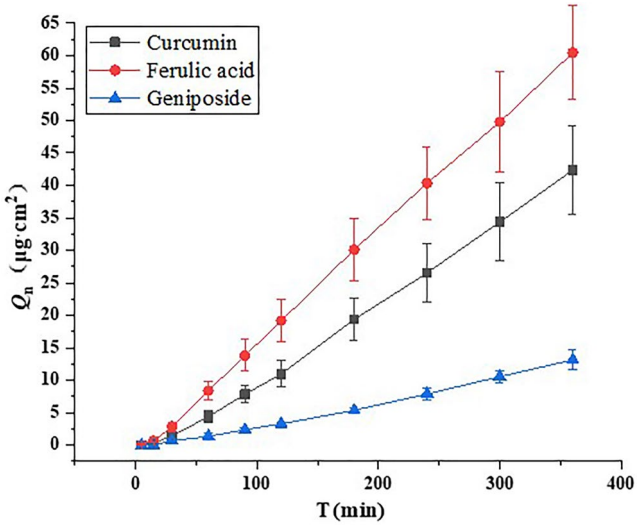

Figure 13. 6 h penetration curves of different nature model drugs in exfoliated skin ($n = 3$).

3.3.3. Effect of MNs and drugs on skin structure

The direct action of MNs and different drugs on the skin surface affects the surface of the SC, and using transmission electron microscopy to observe the changes in the SC and other constituent structures of the skin, the promotion of penetration by MNs and the differences in penetration of different drugs may be reflected by the different effects on the skin structure. From the electron microscopic results (Figure 10), the normal mouse SC is banded, stacked and denser in the outermost layer of the skin. It is this stacked arrangement that curves the interstices of the SC and is partly responsible for the skin having a good permeability barrier. The small protrusions on the outermost layer of the stratum corneum surface were reduced in the solvent group compared to the blank group, indicating that the addition of 80% propylene glycol solvent filled the stratum corneum, but had little effect on its overall results. In the microneedle group at 0 h compared with the blank group, it was evident that the pores left in the epidermal area on the skin after the action of microneedle. A good recovery of the pore depth in the microneedle group at 6 h (Figure 10(C)) compared to the microneedle group at 0 h (Figure 10(J)) can also be found from the transmission electron microscopy. Skin samples with and without MNs action with different nature of drug percutaneous penetration were observed that the drug action basically did not change the skin structure, and the change of skin structure was more obvious after MNs action.

3.3.4. Permeation of drugs with different properties in the pore channel

MNs action on the skin creates many micron-sized pores that break the SC barrier, but there is still an interaction between the drug and the SC during penetration. Therefore, the transdermal process of drug penetration under MNs action is a dual pathway of micropores and transdermal cells, and it is not known which pathway is dominant. From

Table 4. Comparison of MNs action and exfoliation for model drugs pro-permeation ($n = 6$).

Drug	logP	MN		Exfoliation		$ER_{exfoliation}/ER_{MNs}$
		Q_n (μg·cm^{-2})	ER	Q_n (μg·cm^{-2})	ER	
Curcumin	3.62	20.09 ± 6.46	17.43	42.34 ± 6.85	37.05	2.13
Ferulic acid	1.58	40.85 ± 15.35	29.54	60.46 ± 7.23	42.63	1.44
Geniposide	−1.92	10.95 ± 4.17	8.91	13.16 ± 1.55	11.36	1.27

Table 5. Drug SC/media partition coefficients.

Drug	K
Curcumin	0.348 ± 0.021
Ferulic acid	0.180 ± 0.016
Geniposide	0.047 ± 0.037

the results of drug permeation in the pore channels, the permeation amounts of drugs of different properties in the simulated pores of both 0.2 μm microporous filter membrane and microneedle-treated PDMS membrane are: geniposide > curcumin > ferulic acid (Figure 11). The trend of the results of the two pore simulation experiments is the same, but the trend of the results is different from the permeation results of drugs on the skin after MNs action, indicating that the drugs are diffusive in the simulated pores. The difference in drug permeation on the two membranes was huge, with drug permeation on the microporous filter membrane being hundreds of times greater than its permeation on the PDMS membrane. From the perspective of pore size and distribution number, the skin transmission electron microscopy results showed that the pore channels after MNs action were larger than the 0.2 μm pore channels of the microporous filter membrane, except that the porosity on the microporous filter membrane could reach 80%, while the porosity under MNs action was less than 1%, indicating that the difference of drug permeation on the two membranes came from the pore density distribution. Moreover, the drug permeation on the microporous filter membrane is much larger than the drug permeation on the skin under the action of MNs, so the results on the PDMS film are closer to the real pore permeation situation, and the inconsistent trend of the skin permeation experiment under the action of MNs indicates that there are other factors in the skin pore channel.

3.3.5. Lipid exchange of drugs with different properties

Microporous filter membranes and PDMS films only mimic the pore channels left after microneedle action, but when drugs are administered transdermally by microneedle action, there is lipid exchange in the SC in addition to the diffusion effect in the microneedle pore channels (Sloan et al., 2013). The results showed that the permeation of different properties of drugs in Start-M membrane was ferulic acid > curcumin > geniposide (Figure 12). The presence of drug diffusion in the pore channel and the consistent results of drug permeation in the Start-M membrane and mouse skin suggest that drug permeation in the microneedle pore channel is the result of both diffusion and lipid exchange effects. And it can be seen that the pore channel only promotes the increase of drug penetration, and the lipid exchange effect is the main reason for the variability of its percutaneous penetration.

3.4. Mechanistic studies of skin in differential drug penetration

3.4.1. Diffusion of different properties of drugs in exfoliated skin

The SC which is located in the uppermost layer of the skin epidermis is composed of dead keratinocytes as well as the surrounding lipid matrix, and its composition determines that the lipid exchange between the drug and the skin occurs mainly in the SC. but its dense 'brick wall' structure limits the percutaneous penetration of drugs (Boer et al., 2016). In addition, MNs acts by breaking the SC barrier to achieve pro-permeation (Puri et al., 2021), so whether the MNs action is equivalent to the direct removal of the SC and whether drug penetration still differs after removal of the SC. In the experiment, the SC was removed by tape peeling to further investigate the permeation of different drugs on exfoliated skin. From the results, the permeation of different drugs on exfoliated skin was found to be ferulic acid > curcumin > geniposide (Figure 13), the results were consistent with the trend of permeation results of different model drugs under MNs action, indicating that MNs permeation promotion is similar to direct stripping of the SC. Comparising the two methods of MNs and exfoliation for the increased permeation of the model drugs, the results showed that exfoliation was more effective in promoting permeation, as shown in Table 4. As shown by the proinfiltration fold, the proinfiltration fold for curcumin and ferulic acid after exfoliation was approximately twice as high as that after microneedling, while the proinfiltration fold for geniposide was essentially the same. Compared with the two, exfoliation does not significantly improve the transdermal penetration of all drugs, and the direct peeling of the stratum corneum can seriously damage the skin barrier, and its safety is lower compared with the reversible recovery of MNs damage, which is one of the reasons why MNs can be widely used. In addition, the lipid exchange between the drug and the skin was weakened after the removal of the SC, but the trend of drug penetration in the skin before and after the removal was the same, indicating that the lipid exchange effect was overcome and skin structures such as active epidermis and dermis other than the SC were selective for drug penetration. It was further confirmed that breaking the SC barrier is a process to increase the amount of drug penetration, and there is no reversal trend for different properties of drug permeability.

3.4.2. Distribution of different properties of drugs in the SC

The SC is a barrier to transdermal drug penetration, and drugs have to be dissolved in the SC and thus penetrate deeper into the skin (Albery & Hadgraft, 1979). Under the action of MNs to promote permeation, MNs action forms pore channels in

the skin, but the area of the pore channels accounts for less than 1% of the SC area, and the rest of the SC barrier action in the skin remains. How does the permeability of drugs of different properties under MNs correlate with their distribution in the SC. The partition coefficient K of the cuticle/media for each drug as shown in Table 5. The results of the experiment on the distribution of drugs with different properties in the SC were: curcumin > ferulic acid > geniposide, also indicating that the drugs are more lipid soluble and more easily distributed in the SC. This is consistent with the trend of the ratio of the pro-permeation multiplier between removal of the SC and MNs, confirming that the presence of the SC is an important reason for the differences in transdermal permeation of different model drugs. The transdermal permeation of different model drugs under MNs was: ferulic acid > curcumin > geniposide, and the distribution of lipophilic model drug curcumin was the most in the SC, but its transdermal absorption was less relative to ferulic acid, indicating that MNs disrupted the barrier to increase the amount of curcumin into the SC, but the drug accumulated in it, and it was more difficult to enter the lower skin tissues such as hydrophilic active epidermis and dermis with less transdermal absorption. The amphiphilic model drug ferulic acid has an intermediate partition coefficient bureau and its transdermal absorption is the most because its solubility in both the lipophilic SC and the hydrophilic active epidermis and dermis, so the increased drug in the SC can be well absorbed transdermally. Water-soluble geniposide have the least amount of distribution in the SC, and MNs promotion of osmosis increases its drug amount in the SC, and it can't change its difference in lipid solubility with the cells of the SC caused by the difference, so its transdermal absorption is the worst.

4. Conclusion

The results of the combined studies show that MNs have a significant effect on the transdermal penetration of drugs of different properties, and that they are easy to manipulate, painless and convenient to use and more acceptable to patients (Bariya et al., 2012). The results of microneedle facilitation of drug percutaneous penetration showed that small molecules with suitable lipophilic properties are more likely to penetrate percutaneously. In addition, mechanistic studies have shown that MNs promote transdermal drug penetration by breaking the SC barrier, while microneedle pores don't alter the drug-skin interaction, but only enhance the diffusion of the drug. However, its barrier-breaking effect is reversible and safer than direct stripping of the SC. Differences in the permeability of drugs of different properties are also reflected in differences in the transdermal route, and MNs increase the amount of drug distribution when it promotes drug permeation without altering the transdermal route. This study proposes a new idea for the study of solid microneedle permeation promotion from multiple perspectives such as microneedle pores and skin structure, and provides a reference for the selection of appropriate physical permeation promotion for drugs of different properties.

Acknowledgments

We would like to thank everyone who contributed to this article. We would also like to thank the reviewers for their valuable comments.

Author contributions

Investigation, Data Curation and Writing-Original Draft (Huahua Li); Formal Analysis (Ziwei Peng, Yang Song, Minhang Dou and Xinying Lu); Methodology (Minghui Li, Xiaofeng Zhai, Yan Gu, Rexidanmu·Mamujiang); Funding Acquisition (Shouying Du and Jie Bai); Writing-Review and Editing (Jie Bai).

Data availability

Data will be made available on request.

Disclosure statement

No potential conflict of interest was reported by the author(s).

Ethics of experimentation

All animal studies were performed under the Guidelines for the Care and Use of Laboratory Animals, and experimental protocols were approved by the institutional animal experimentation committee of Beijing University of Chinese Medicine.

Funding

This work was supported by the Fundamental Research Funds for the Central Universities [grant number 2020-JYB-ZDGG-031].

References

Abla N, Naik A, Guy RH, et al. (2005). Contributions of electromigration and electroosmosis to peptide iontophoresis across intact and impaired skin. J Control Release 108:1–11.

Albery WJ, Hadgraft J. (1979). Percutaneous absorption: in vivo experiments. J Pharm Pharmacol 31:140–7.

Barbero AM, Frasch HF. (2006). Transcellular route of diffusion through stratum corneum: results from finite element models. J Pharm Sci 95:2186–94.

Bariya SH, Gohel MC, Mehta TA, et al. (2012). Microneedles: an emerging transdermal drug delivery system. J Pharm Pharmacol 64:11–29.

Barry BW, Bennett SL. (1987). Effect of penetration enhancers on the permeation of mannitol, hydrocortisone and progesterone through human skin. J Pharm Pharmacol 39:535–46.

Benfeldt E. (1999). In vivo microdialysis for the investigation of drug levels in the dermis and the effect of barrier perturbation on cutaneous drug penetration. Studies in hairless rats and human subjects. Acta Derm Venereol Suppl (Stockh) 206:1–59.

Boer M, Duchnik E, Maleszka R, et al. (2016). Structural and biophysical characteristics of human skin in maintaining proper epidermal barrier function. Postepy Dermatol Alergol 33:1–5.

Cadavona JJ, Zhu H, Hui X, et al. (2016). Depth-dependent stratum corneum permeability in human skin in vitro. J Appl Toxicol 36:1207–13.

Chang SL, Hofmann GA, Zhang L, et al. (2000). The effect of electroporation on iontophoretic transdermal delivery of calcium regulating hormones. J Control Release 66:127–33.

Chen X, Zhu L, Li R, et al. (2020). Electroporation-enhanced transdermal drug delivery: Effects of logP, pKa, solubility and penetration time. Eur J Pharm Sci 151:105410.

Guillot AJ, Cordeiro AS, Donnelly RF, et al. (2020). Microneedle-based delivery: an overview of current applications and trends. Pharmaceutics 12:569.

Haq A, Goodyear B, Ameen D, et al. (2018). Strat-M® synthetic membrane: permeability comparison to human cadaver skin. Int J Pharm 547:432–7.

Haque T, Talukder MMU. (2018). Chemical enhancer: a simplistic way to modulate barrier function of the stratum corneum. Adv Pharm Bull 8:169–79.

Kováčik A, Kopečná M, Vávrová K. (2020). Permeation enhancers in transdermal drug delivery: benefits and limitations. Expert Opin Drug Deliv 17:145–55.

Kovács A, Zsikó S, Falusi F, et al. (2021). Comparison of synthetic membranes to heat-separated human epidermis in skin permeation studies in vitro. Pharmaceutics 13:2106.

Lan Y, Wang JY, Tao Y, et al. (2016). Comparison of essential oil from *Mentha haplocalyx* and menthol used as penetration enhancers. Zhongguo Zhongyao Zazhi 41:1516–22 (in Chinese).

Marwah H, Garg T, Goyal AK, et al. (2016). Permeation enhancer strategies in transdermal drug delivery. Drug Deliv 23:564–78.

Mdanda S, Ubanako P, Kondiah PPD, et al. (2021). Recent advances in microneedle platforms for transdermal drug delivery technologies. Polymers (Basel) 13:2405.

Mitragotri S, Kost J. (2004). Low-frequency sonophoresis: a review. Adv Drug Deliv Rev 56:589–601.

Montenegro L, Lai F, Offerta A, et al. (2016). From nanoemulsions to nanostructured lipid carriers: a relevant development in dermal delivery of drugs and cosmetics. J. Drug Deliv. Sci. Technol 32:100–12.

Parhi R, Suresh P, Patnaik S. (2015). Physical means of stratum corneum barrier manipulation to enhance transdermal drug delivery. Curr Drug Deliv 12:122–38.

Prausnitz MR, Langer R. (2008). Transdermal drug delivery. Nat Biotechnol 26:1261–8.

Puri A, Nguyen HX, Tijani AO, et al. (2021). Characterization of microneedles and microchannels for enhanced transdermal drug delivery. Ther Deliv 12:77–103.

Riemma Pierre M, Rossetti F. (2014). Microneedle-based drug delivery systems for transdermal route.[J. CDT 15:281–91.

Sarango-Granda P, Espinoza LC, Díaz-Garrido N, et al. (2022). Effect of penetration enhancers and safety on the transdermal delivery of apremilast in skin. Pharmaceutics 14:1011.

Seah BC, Teo BM. (2018). Recent advances in ultrasound-based transdermal drug delivery. Int J Nanomedicine 13:7749–63.

Sloan KB, Synovec J, Ketha H. (2013). A surrogate for topical delivery in human skin: silicone membranes. Ther Deliv 4:203–24.

Waghule T, Singhvi G, Dubey SK, et al. (2019). Microneedles: a smart approach and increasing potential for transdermal drug delivery system. Biomed Pharmacother 109:1249–58.

Xie F, Chai JK, Hu Q, et al. (2016). Transdermal permeation of drugs with differing lipophilicity: effect of penetration enhancer camphor. Int J Pharm 507:90–101.

Yang HJ, Huang JY, Yang YL, et al. (2021). Orthogonal experiments combined with OCT for optimal microneedling conditions of cinnamaldehyde liposome transdermal. Chin J Pharmacol 56:738–43.

Yang L, Wu L, Wu D, et al. (2017). Mechanism of transdermal permeation promotion of lipophilic drugs by ethosomes. Int J Nanomed 12:3357–64.